Chemistry Letters

http://www.csj.jp/journals/chem-lett/

Vol.33 No.12
December, 2004

CMLTAG
ISSN 0366-7022

Highlight Review

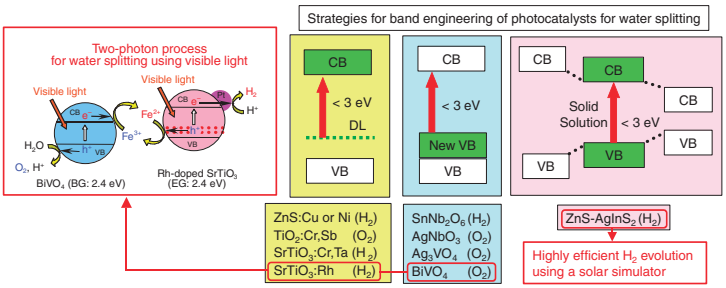

Photocatalysts for water splitting developed by the present authors are reviewed. A NiO (0.2 wt %)/$NaTaO_3$:La (2%) photocatalyst with a 4.1-eV band gap showed high activity for water splitting into H_2 and O_2 with an apparent quantum yield of 56% at 270 nm. Many visible-light-driven photocatalysts have also been developed through band engineering by doping of metal cations, forming new valence bands with Bi_{6s}, Sn_{5s}, and Ag_{4d} orbitals, and by making solid solutions between ZnS with wide band gap and narrow band gap semiconductors. Overall water splitting under visible light irradiation has been achieved by construction of a Z-scheme photocatalysis system employing the visible-light-driven photocatalysts for H_2 and O_2 evolution, and the Fe^{3+}/Fe^{2+} redox couple as an electron relay.

Letter

Polarization curves for oxygen reduction in 10 M NaOH under an air atmosphere at room temperature.

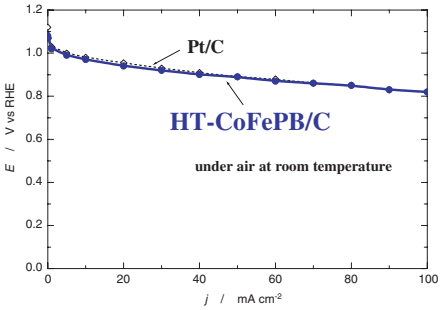

1542 **Effects of Pressure on the Thermal Back Electron Transfer in a Dibenzylbipyridinium Salt. Solvent Reorganizations and Dynamic Solvent Effects**

Mehdi S. Shihab, Koji Kubota, Toru Takahashi, Yasushi Ohga, and Tsutomu Asano

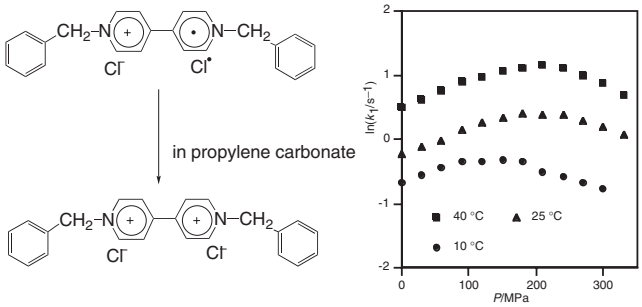

1544 **Photochemical and Enzymatic Synthesis of Methanol from HCO_3^- with Dehydrogenases and Zinc Porphyrin**

Yutaka Amao and Tomoe Watanabe

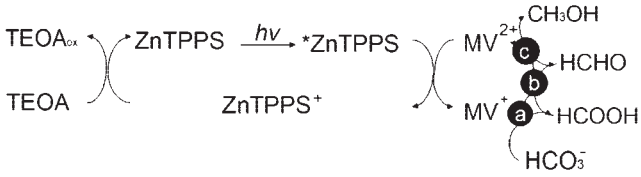

Photochemical and enzymatic methanol synthesis from HCO_3^- with formate (a), aldehyde (b), and alcohol dehydrogenases (c) via the photoreduction of methylviologen (MV^{2+}) using zinc porphyrin (ZnTPPS) photosensitization.

1546 **Formation of TaC Nanorods with a Low-Temperature Chemical Route**

Liang Shi, Yunle Gu, Luyang Chen, Zeheng Yang, Jianhua Ma, and Yitai Qian

$$4TaCl_5 + C_4Cl_6 + 26Na \xrightarrow{650\ ^\circ C} 4TaC + 26NaCl$$

1548 **Porous TiO_2 (anatase) Electrodes for High-Power Batteries**

Hirotoshi Yamada, Takanori Yamato, Isamu Moriguchi, and Tetsuichi Kudo

Scanning electron micrographs of Au-supported films of (left) bimodal PS colloid assembly and (right) bimodal porous TiO_2, prepared by using PS colloids with diameters of 50 and 430 nm.

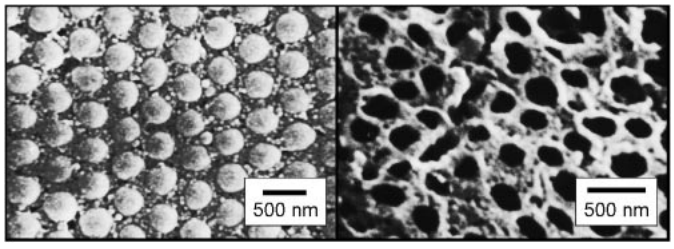

1550 **Gene Detection Based on the Tetrakis-acridinyl Peptide (TAP) Cassette**

Keiji Mizuki, Takahiko Nojima, and Shigeori Takenaka

The tetrakis-acridinyl peptide (TAP) cassette, formed by the reaction of TAP with an oligonucleotide carrying a continuous AT sequence, was used for the detection of target DNA by the sandwich assay on the titer plate.

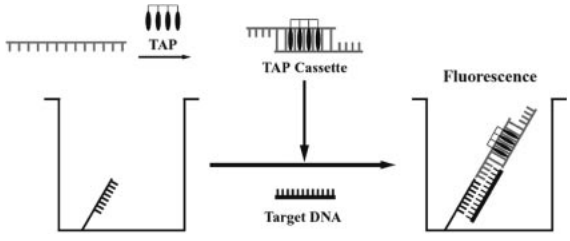

1552 **Preparation of Biodegradable Hollow Nanocapsules by Silica Template Method**

Yuki Itoh, Michiya Matsusaki, Toshiyuki Kida, and Mitsuru Akashi

Biodegradable hollow nanocapsules were successfully prepared by a combination of layer-by-layer assembly and the silica template method.

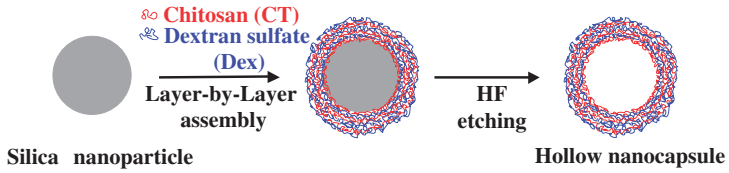

1554 **Introduction of Peptide Functions into DNA by Nucleic Acid Peptides, NAPs**

Junji Kawakami, Zhong-Ming Wang, Hiroyoshi Fujiki, Satoshi Izumi, and Naoki Sugimoto

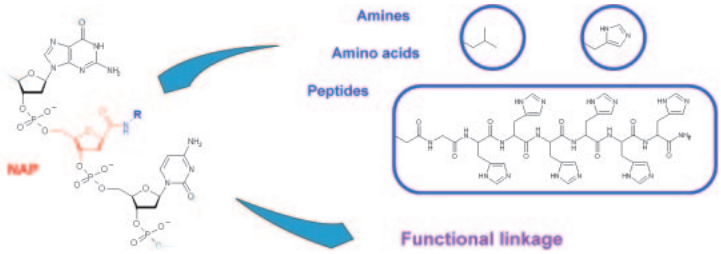

1556 **Thermal Stability of Mononuclear Hydroperoxocopper(II) Species. Effects of Hydrogen Bonding and Hydrophobic Field**

Syuhei Yamaguchi, Akira Wada, Shigenori Nagatomo, Teizo Kitagawa, Koichiro Jitsukawa, and Hideki Masuda

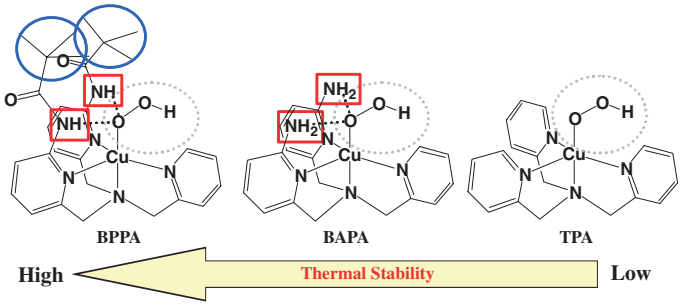

1558 **Effect of Cetyldimethylbetaine Molecules on Agglomeration and Growth of Ice**

Poly R. Modak, Hiromoto Usui, Hiroshi Suzuki, and Takaaki Inada

Certain surfactants with suitable brine, such as cetyldimethylbetaine with sorbitol, can inhibit agglomeration of ice particles and thus help disperse ice particles in ice/water slurries, and simultaneously reduce the drag of the slurry in pipes. In this study, the amount of cetyldimethylbetaine (surfactant) molecules remaining in the liquid phase of ice/water slurries was measured. Then, on the basis of these measurements, models to explain how these cetyldimethylbetaine molecules affect ice to inhibit agglomeration of ice particles were proposed.

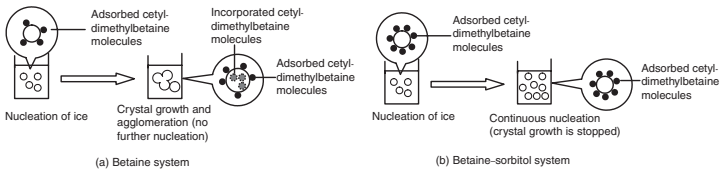

1560 **Multiwalled Carbon Nanotubes/Co_3O_4 Nanocomposites and Its Electrochemical Performance in Lithium Storage**

Yan Shan and Lian Gao

Multiwalled carbon nanotubes coated with a thick layer of Co_3O_4 nanocrystals are prepared. The coating layer is 15–20 nm in thickness and composed of Co_3O_4 with an average size of 8 nm. The MWWNTs/Co_3O_4 composites have larger lithium storage capacities and a better cycle-ability, and have potential use in Li ion battery materials.

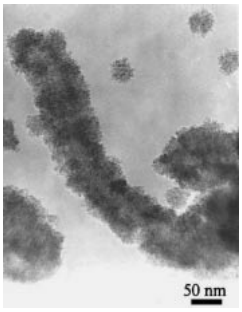

1562 **The Preparation of TiO_2 Nanoparticle Photocatalysts by a Flame Method and Their Photocatalytic Reactivity for the Degradation of 2-Propanol**

Bernaurdshaw Neppolian, Hyun Seock Jie, Jae-Pyoung Ahn, Jong-Ku Park, and Masakazu Anpo

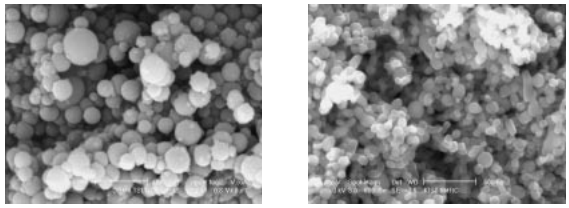

SEM images of Fe–TiO_2 (left) and FeZn–TiO_2 bimetal incorporated (right) photocatalysts.

1564 **Synthesis of Nickel Nanocrystallites with Hexagonal Flake-like Morphology from Nickel Dimethylglyoximate**

Xiaomin Ni, Lifu Chen, Huagui Zheng, Dongen Zhang, Qingbiao Zhao, and Jimei Song

Nickel nanocrystallites with hexagonal flake-like morphology, having a side length of 200–400 nm and a thickness of 20–30 nm, were prepared by reduction of nickel dimethylglyoximate with hydrazine hydrate in a solution. The precursor of nickel dimethylglyoximate played an important role for the formation of single crystalline flakes.

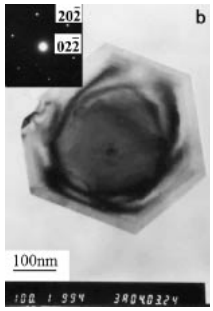

1566 **Successive Phase Transitions in Crystalline State of Mesogenic Butyl 4-[2-(Perfluorooctyl)ethoxy]benzoate**

Minako Maeda, Motoi Nagasawa, Makoto Tachibana, Hitoshi Kawaji, Tooru Atake, Akifumi Iida, Tomoji Ozeki, and Kayako Hori

Successive L–M–H phase transitions associated with the change of the periodicity of molecular stacking in the monoclinic unit cell of $Z = 12$, 16, and 4 for L, M, and H phases, respectively.

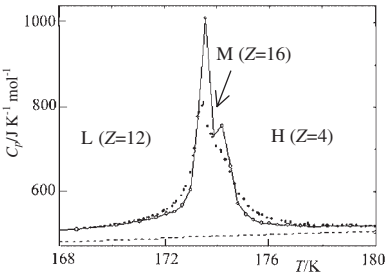

1568 **Sensitized Photoluminescence of Eu^{3+} and Gd^{3+}-Doped $Y_3Al_5O_{12}$ Phosphors Prepared via a Reverse Microemulsion Process**

Chung-Hsin Lu and Chien-Hao Huang

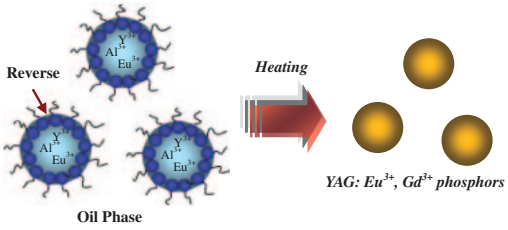

Well-dispersed europium-ion and gadolinium-ion codoped yttrium aluminum garnet (YAG: Eu^{3+}, Gd^{3+}) phosphors have been successfully prepared via a newly developed water-in-oil microemulsion process. This microemulsion process not only significantly shortens the reaction time for preparing phase-pure YAG, but also decreases the particle size of YAG: Eu^{3+}, Gd^{3+} to submicron order.

1570 **Preparation and Properties of 1,2-Bis[(2,4,6-tri-*t*-butylphenyl)phosphinidene]cyclobuta-[*l*]phenanthrene**

Akitake Nakamura, Subaru Kawasaki, Kozo Toyota, and Masaaki Yoshifuji

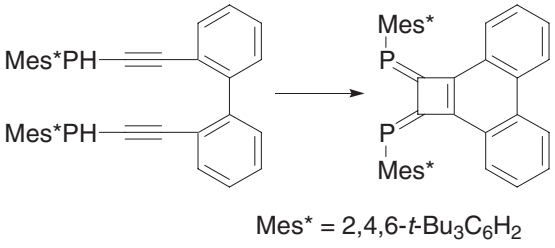

Mes* = 2,4,6-*t*-$Bu_3C_6H_2$

1572 **Novel Layered Organic–Inorganic Networks Assembled From PbI_2 and *N*,*N*′-bis(3-pyridylmethyl)-1,4-biphenylenedimethyleneimine**

Ling-Yan Kong, Zheng-Hua Zhang, Taka-aki Okamura, Ming-Jian Fei, Wei-Yin Sun, and Norikazu Ueyama

Two novel metal-organic frameworks with different structures were obtained by reactions of PbI_2 with *N*,*N*′-bis(3-pyridylmethyl)-1,4-biphenylenedimethyleneimine (L) under different M/L ratios.

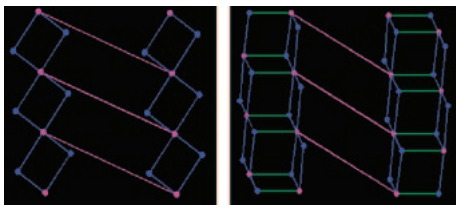

1574 **Synthesis of Carbon Nanofoams and Nanospheres by Varying Ratio of Phenol–Formaldehyde Resin to Mesoporous Silica Foams**

Dong-Wun Chen, Chun-Yi Chang-Chien, Hong-Ping Lin, Yen-Po Lin, and Chin-Yuan Tang

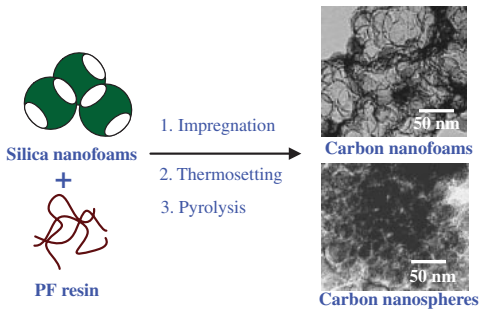

1576 **Platinum Thin Film with a Highly Ordered Mesostructure by Contact Plating**

Yusuke Yamauchi, Tokihiko Yokoshima, Toshiyuki Momma, Tetsuya Osaka, and Kazuyuki Kuroda

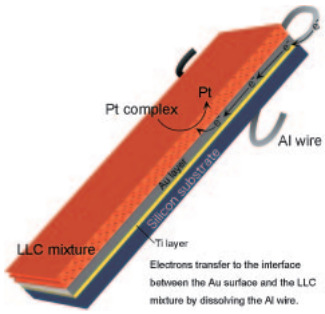

1578 **Templateless Hydrothermal Synthesis of Aligned ZnO Nanorods**

Yongnan Zhao and Young-Uk Kwon

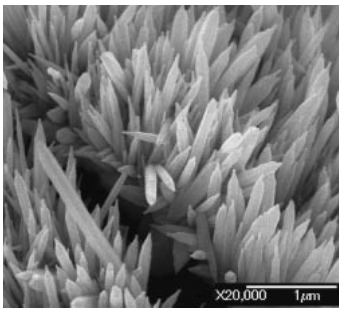

1580 **Formation of $[Cu(\eta^2\text{-}H_2)]^+$ Species in MFI-type Zeolite and Resulting H–D Exchange Reaction with Hydrogen on Brønsted Acid Sites at 300 K**

Yasushige Kuroda, Takae Okamoto, Toshinori Mori, and Yuzo Yoshikawa

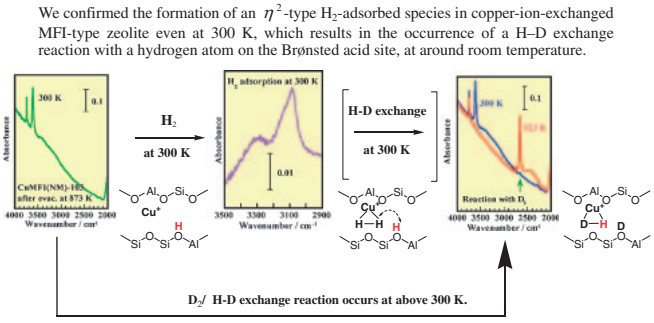

1582 **Aminopropyl–Glucose Sequentially Grafted Mesoporous Silica Nanocomposite as a Novel Boron Adsorbent**

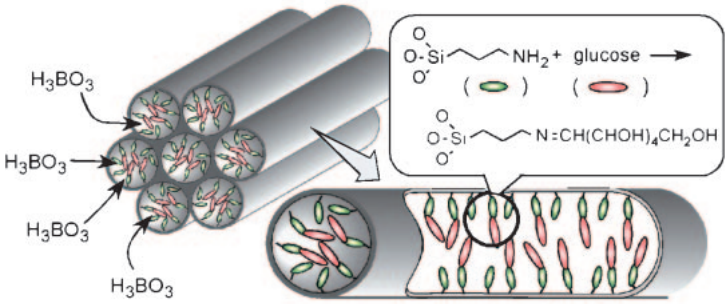

Masataka Yasui, Masataka Ikeda, Kazuo Takimiya, Joji Ohshita, Shoji Yamanaka, and Kei Inumaru

1584 **Dansylation of Endocrine-disrupting Alkylphenolic Compounds on the Solid Phase Used for Extraction from Environmental Water**

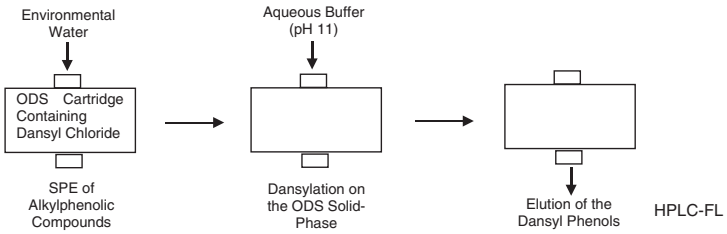

Bunji Uno, Jiro Katsumi, and Kazumi Aoki

1586 **In Situ Ligand Synthesis for a Novel 1-D Mn Coordination Polymer**

A novel coordination polymer, $[Mn(II)(HL)_2]_n$ (H_2L = 4-hydroxynicotinic acid) was hydrothermally synthesized. Interestingly, an in situ ligand synthesis for HL from 3,4- pyridinedicarboxylic acid precursor was observed. Its structure is built up from Mn(II)-centered octahedron and HL ligand. The μ_3-HL ligand plays dual roles for the formation of 1-D framework: chelate and bridge.

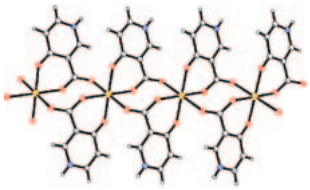

Ding Weng, Yude Wang, Ranbo Yu, Ruji Wang, Dan Wang, Qiang Cai, Hengde Li, and Youwei Yao

1588 **One-pot Synthesis of Furo[3,2-*c*]oxepin-4-one Derivatives by the CAN-mediated Reaction of *tert*-Butyl 2-(2-Hydroxytetrahydrofuran-2-yl)acetates with Alkenes**

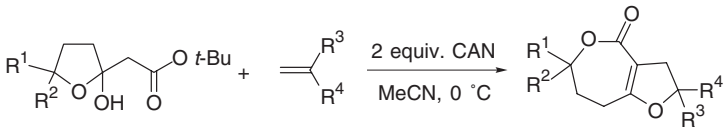

R^1, R^2 = H, alkyl ,Ph R^3, R^4 = alkyl, aryl

Kazuhiro Kobayashi, Hironobu Umakoshi, Kazutaka Hayashi, Osamu Morikawa, and Hisatoshi Konishi

1590 **Discovery of a Magnetic Ionic Liquid [bmim]$FeCl_4$**

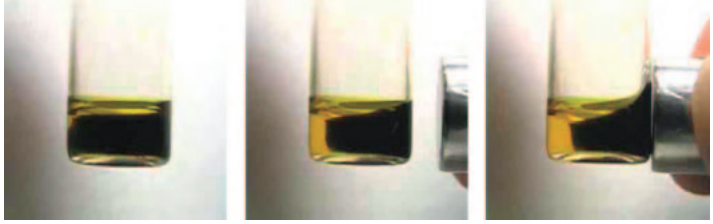

Satoshi Hayashi and Hiro-o Hamaguchi

A magnetic ionic liquid, which responds strongly to a magnet, has been discovered.

1592 **Cross Metathesis Route in Sphingomyelin Synthesis**

Hiroko Hasegawa, Tetsuya Yamamoto, Sho Hatano, Toshikazu Hakogi, and Shigeo Katsumura

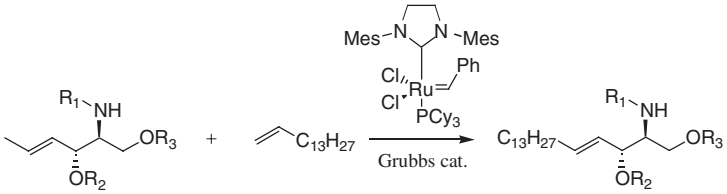

1594 **A New Family of Zwitterionic Liquids Arising from a Phase Transition of Ammonium Inner Salts Containing an Ether Bond**

Masahiro Yoshizawa and Hiroyuki Ohno

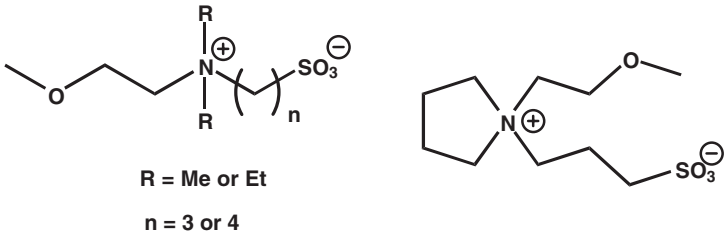

1596 **Redox Behavior of New Ru–Dioxolene–Ammine Complexes and Catalytic Activity toward Electrochemical Oxidation of Alcohol under Mild Conditions**

Takami Hino, Tohru Wada, Tetsuaki Fujihara, and Koji Tanaka

New Ru–dioxolene–ammine complex, $[Ru^{II}(NH_3)(sq)(trpy)](ClO_4)$ (**1**), has an ability to oxidize *i*-PrOH catalytically under very mild conditions such as the electrolysis at 0 V (vs SCE) in CH_2Cl_2.

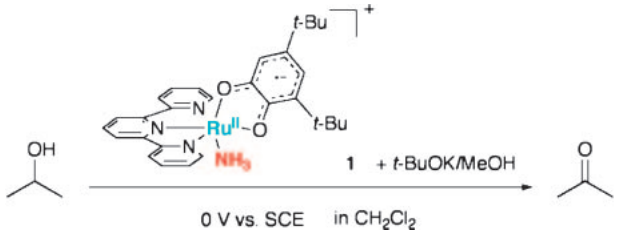

1598 **Preparation and Photocurrent Generation of Nanostructured SnO_2 Films Chemically Modified with Mono-substituted C_{60}-Malonic Acid**

Hideo Ohkita, Yuta Shimazaki, Masataka Ohoka, and Shinzaburo Ito

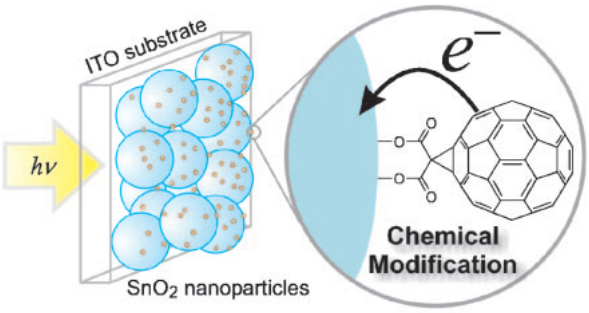

1600 **Pathway to Insoluble Aggregates on the Refolding of a Single-chain Fv Antibody: Morphological Changes of Aggregated Protein on Refolding**

Mitsuo Umetsu, Kumar Ashish, Kouhei Tsumoto, and Izumi Kumagai

The temperature applied for refolding of single-chain Fv antibodies is critical to the morphology of the aggregated form.

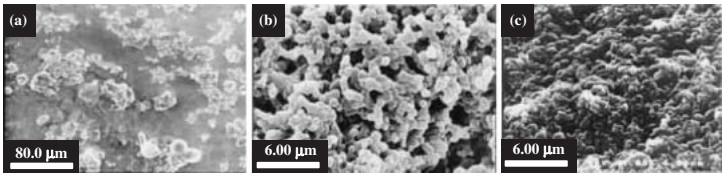

1602 **Colloidal Nanoparticles from Poly(*N*-isopropylacrylamide)-*graft*-DNA for Single Nucleotide Discrimination Based on Salt-induced Aggregation: Extension to Long Target DNA**

Zhonglan Tang, Tohru Takarada, Yoshikuni Sato, and Mizuo Maeda

Single nucleotide difference of 39-mer target DNA has been detected successfully by using colloidal nanoparticles formed from the copolymer. The nanoparticles aggregated rapidly in the presence of the full match DNA, while dispersed in the presence of the mismatch one.

1604 **Efficient Acetalization of Epoxy Rings on a Fullerene Cage**

Yasuo Shigemitsu, Masayoshi Kaneko, Yusuke Tajima, and Kazuo Takeuchi

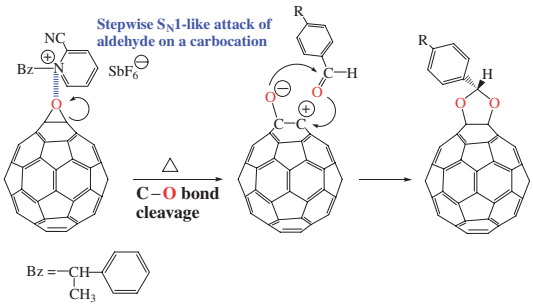

1606 **Novel Dinuclear Copper(II) Complexes with *syn–syn* and *syn–anti* Coordination Modes of Bis(μ-phosphinato)-bridges: Structures and Magnetic Properties**

Koichi Koga, Miki Ohtsubo, Yasunori Yamada, Masayuki Koikawa, and Tadashi Tokii

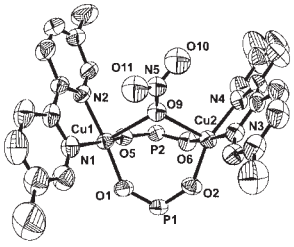

$[Cu_2(NO_3)(bmp)_2(5\text{-dmbpy})_2]^+$ (**1**)

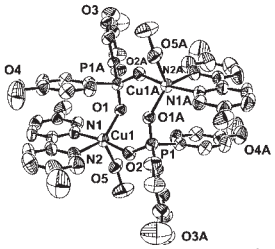

$[Cu_2(bmp)_2(5\text{-dmbpy})_2(MeOH)_2]^{2+}$ (**2**)

1608 **Synthesis of Novel Nanocrystals as Fluorescent Sensors for Hg^{2+} Ions**

Bo Chen, Ying Yu, Zhentao Zhou, and Ping Zhong

CdTe nanocrystals (NCs) were synthesized to be used as fluorescent sensors for selectively detecting Hg^{2+} ions. The surface binding of Hg^{2+} ions with different concentrations quenched the fluorescence of NCs possibly owing to the effective electron transfer from MPA to Hg^{2+} ions and the facilitation of nonradiative recombination of excited electrons (e^-) in the conduction band and holes (h^+) in the valence band.

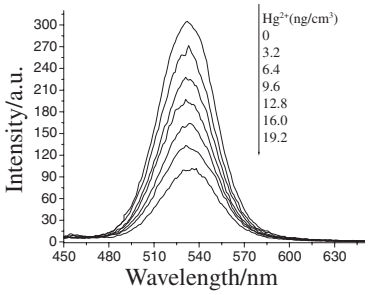

1610 **Oxidation of Aldehydes on TiO_2 Photocatalysts Modified with Alkylsilyl Group**

Teruhisa Ohno, Toshiki Tsubota, Kosuke Kakiuchi, and Kazuhiro Sayama

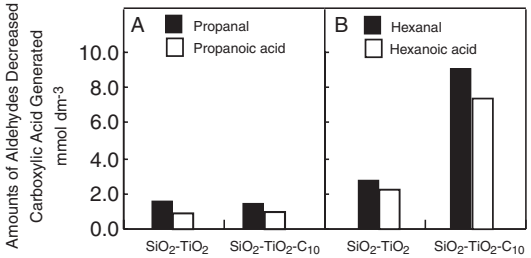

Oxidation of hexanal on surface modified TiO_2 (SiO_2–TiO_2–C_{10}) proceeded more efficiently than that on TiO_2 without surface modification (SiO_2–TiO_2).

1612 **Hydrothermal Synthesis of a Novel Sodium Vanadium Bronze with Single-crystalline Nanobelt-like Morphology**

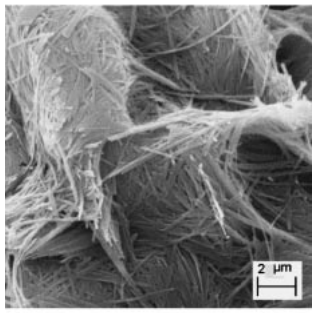

Gen-Tao Zhou, Xin-Chen Wang, and Jimmy C. Yu

1614 **CsOH·H_2O-Promoted Synthesis of Aryl Sulfides via Direct Coupling of Aryl Halides and Thiols**

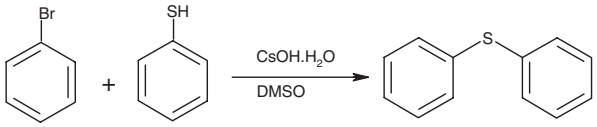

(17 examples)

Ravi Varala, E. Ramu, M. Mujahid Alam, and Srinivas R. Adapa

1616 **A Templated Bimetallic Phosphate Open-structure with 16-MR Channels**

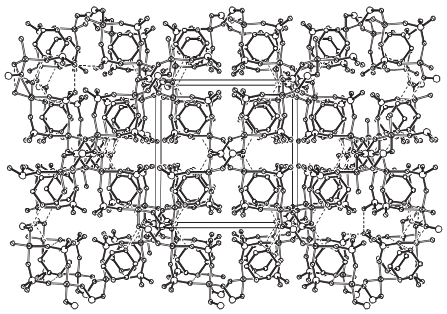

Wei Chen, Yongnan Zhao, and Young-Uk Kwon

1618 **Long-Term Sampling Method for PCDD/Fs in Atmosphere by Adsorption onto Economical Materials**

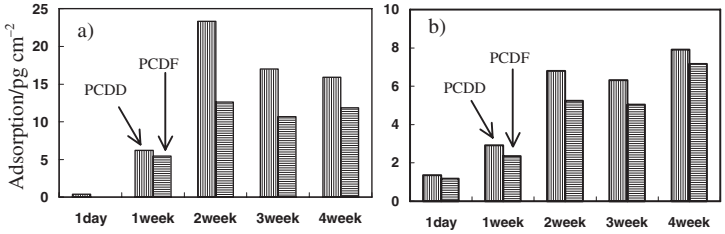

Adsorption amount of PCDD/Fs onto polyurethane foam on the various sampling period. (a), spring season; (b) autumn season.

Hideyuki Katsumata, Satoshi Kaneco, Tohru Suzuki, and Kiyohisa Ohta

1620 **Formation of Niobates from Aqueous Peroxide Solution**

$$K(Li)OR + H_2O + Nb(OR)_5 \rightarrow K(Li)-O-Nb$$

$$K(Li)-O-Nb + H_2O_2 \rightarrow K(Li)-O-O-Nb$$

$$K(Li)-O-O-Nb \xrightarrow{annealing} K(Li)NbO_3$$

Peroxide prepared through the reaction of aqueous hydrogen peroxide solution with metal alkoxide is a promising precursor for niobates thin film and powder.

Zhenxiang Cheng, Kiyoshi Ozawa, Akimitsu Miyazaki, and Hideo Kimura

1622 **Porous/Disk-dual Microelectrode: Preparation and Electrochemical Detection of Methanol Electrooxidation Product at Pt/C Powder Electrocatalyst**

Kohshi Kashima, Minoru Umeda, Akifumi Yamada, and Isamu Uchida

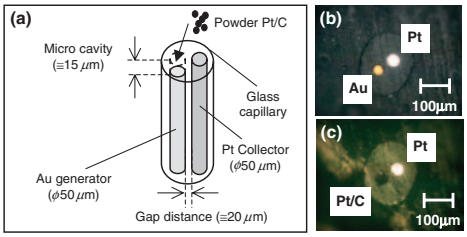

Schematic illustration (a) and optical micrographs of porous/disk-dual microelectrode at the tip packed with (c) and without (b) Pt/C powder.

1624 **Synthesis of an Electron Pooling Ligand Based on Triruthenium Clusters and Electrochemical Reduction of CO_2 by Its Zinc(II) Complex**

Brian K. Breedlove, Daisuke Takayama, and Tasuku Ito

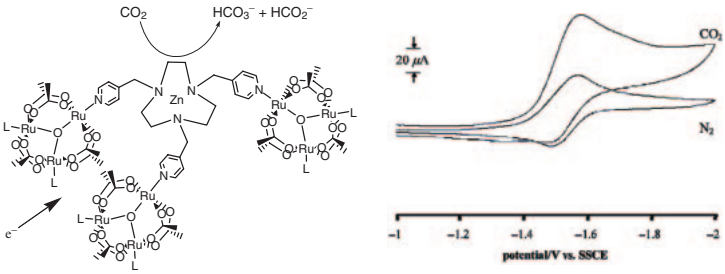

1626 **TTMPP Catalyzed One-pot Silyl Ketene Acetal–Imine Condensation Route to β-Lactams**

Satoru Matsukawa and Kayoko Obu

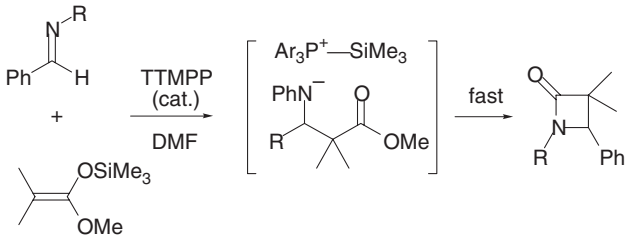

1628 **Vapor-Phase Dehydrogenation of Methanol to Methyl Formate in Catalytic Membrane Reactor with Pd/SiO_2/Ceramic Composite Membrane**

Yanglong Guo, Guanzhong Lu, Xunhua Mo, and Yunsong Wang

Vapor-phase dehydrogenation of methanol to methyl formate was investigated in the catalytic membrane reactor (CMR) with the Pd/SiO_2/ceramic composite membrane. The studies show that the CMR has much better performance than the fixed-bed reactor under the similar reaction conditions. In the CMR, the selectivity of methyl formate is close to 100% at 60–150 °C, and the maximum conversion of methanol (19.5%) is achieved at 90 °C. In the fixed-bed reactor, the conversion of methanol is nearly zero and no methyl formate is detected in the effluent.

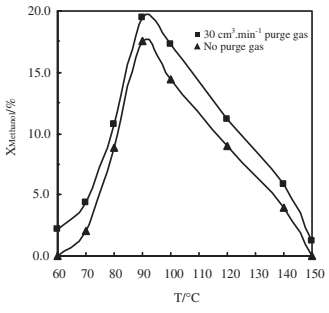

1630 **Effect of Methyl Groups onto Imidazolium Cation Ring on Liquid Crystallinity and Ionic Conductivity of Amphiphilic Ionic Liquids**

Tomohiro Mukai, Masafumi Yoshio, Takashi Kato, and Hiroyuki Ohno

Asymmetric imidazolium dodecylsulfonate showed large hysteresis in the ionic conductivity reflecting monotropic liquid crystallinity.

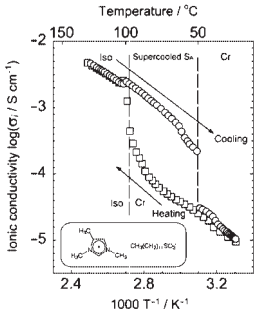

1632 **Novel Field-effect Transistors Based on Bis(1,3-dithiol-2-ylidene) Compounds with a Conjugated Spacer Group**

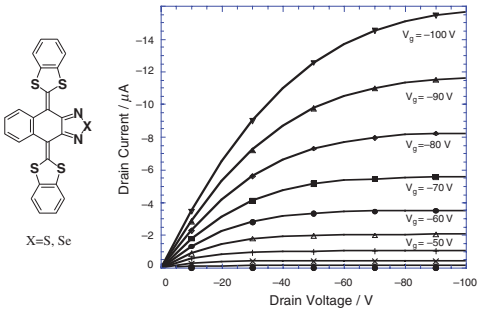

Yosuke Morioka, Jun-ichi Nishida, Eiichi Fujiwara, Hirokazu Tada, and Yoshiro Yamashita

1634 **Precise Determination of the Atmospheric CF_4 Concentration by Using Natural Kr in the Atmosphere as an Internal Reference in the Preconcentration/GC/MS Analysis**

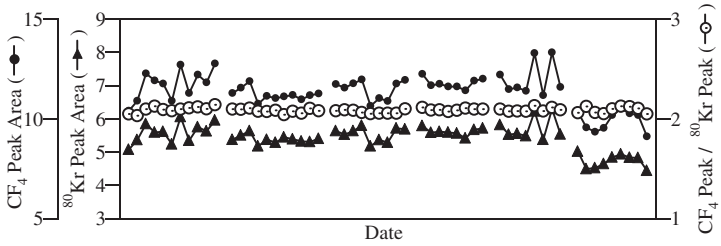

Nobuyuki Aoki and Yoshihiro Makide

1636 **Low-melting, Low-viscous, Hydrophobic Ionic Liquids: *N*-Alkyl(alkyl ether)-*N*-methylpyrrolidinium Perfluoroethyltrifluoroborate**

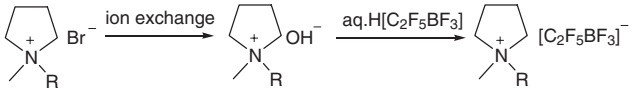

R = *n*-C_mH_{2m+1} (*m* = 3–7), CH_3OCH_2, $CH_3O(CH_2)_2$, $C_2H_5O(CH_2)_2$, $CH_3O(CH_2)_2O(CH_2)_2$

Zhi-Bin Zhou, Hajime Matsumoto, and Kuniaki Tatsumi

1638 **Novel SiO_2 Nanotubes: Synthesis from ZnS Nanowires Templates and Visible Photoluminescence at 615 nm**

The novel silica nanotubes with flower-like morphology and hexagonal outer surface morphology were fabricated via a simple ZnS nanowires templates-assisted CVD method.

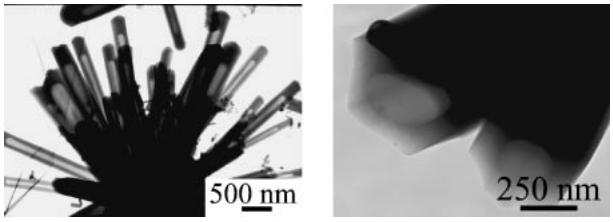

Yan Li, Chang-Hui Ye, Li-De Zhang, Xiao-Sheng Fang, and Yu-Gang Zhang

1640 **Long-range Ordering in Water–Halide Ion Interactions: A Database Study**

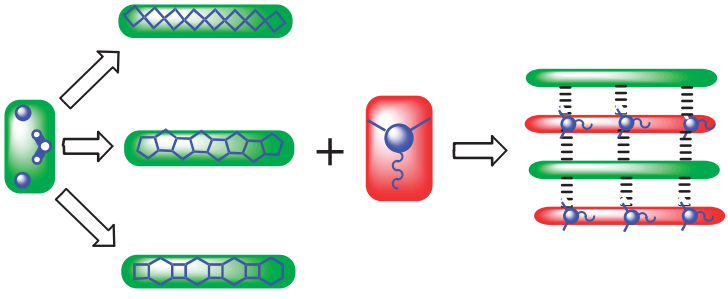

Ponraj Prabakaran and Maria G. Singarayan

